



ZnO Quantum Dots Induced Oxidative Stress and Apoptosis in HeLa and HEK-293T Cell Lines

Yanjie Yang, Zhenhua Song, Weixia Wu, Ao Xu, Shuangyu Lv* and Shaoping Ji*

Provincial Engineering Centre for Tumor Molecular Medicine, School of Basic Medical Sciences, Henan University, Kaifeng, China

OPEN ACCESS

Edited by:

Eleonore Fröhlich,
Medical University of Graz, Austria

Reviewed by:

Nelson Marmioli,
University of Parma, Italy
Guimiao Lin,
Shenzhen University, China

*Correspondence:

Shuangyu Lv
shuangyulv@163.com
Shaoping Ji
shaopingji@henu.edu.cn

Specialty section:

This article was submitted to
Predictive Toxicology,
a section of the journal
Frontiers in Pharmacology

Received: 16 November 2019

Accepted: 30 January 2020

Published: 27 February 2020

Citation:

Yang Y, Song Z, Wu W, Xu A,
Lv S and Ji S (2020) ZnO
Quantum Dots Induced Oxidative
Stress and Apoptosis in HeLa
and HEK-293T Cell Lines.
Front. Pharmacol. 11:131.
doi: 10.3389/fphar.2020.00131

Zinc oxide (ZnO) quantum dot (QD) is a promising inexpensive inorganic nanomaterials, of which potential toxic effects on biological systems and human health should be evaluated before biomedical application. In this study, the cytotoxicity of ZnO QDs was assessed using HeLa cervical cancer cell and HEK-293T human embryonic kidney cell lines. Cell viability was significantly decreased by treatment with 50 $\mu\text{g/ml}$ ZnO QDs after only 6 h, and the cytotoxicity of ZnO QDs was higher in HEK-293T than in HeLa cells. ZnO QDs increased the level of reactive oxygen species and decreased the mitochondria membrane potential in a dose-dependent manner. Several gene expression involved in apoptosis was regulated by ZnO QDs, including bcl-2 gene and caspase. In HeLa cells, ZnO QDs significantly increased early and late apoptosis, but only late apoptosis was affected in HEK-293T cells. These findings will be helpful for future research and application of ZnO QDs in biomedicine.

Keywords: ZnO quantum dots, cytotoxicity, reactive oxygen species, mitochondria membrane potential, apoptosis

INTRODUCTION

Zinc oxide nanoparticles (ZnO NPs) are one of the most extensively used nanomaterials, due to the unique physicochemical properties and low cost. ZnO NPs could protect the cells against the ultraviolet (UV)-induced skin damage, and have been applied to cosmetics (Vallabani et al., 2019). ZnO NPs are used in the packaging and food industry as additives owing to their antimicrobial properties (Sharma et al., 2012; Kim et al., 2019). ZnO NPs are also being explored for biomedical applications, including pharmaceuticals, dental fillings, drug delivery, biosensors, and bioimaging (Kim et al., 2019; Vallabani et al., 2019). With the expanded production and application of ZnO NPs, the concerns of their potential toxicity in human health and environmental safety have raised (Song et al., 2019). ZnO NPs were reported to induce cytotoxicity in a variety of cancer cells, including HepG2, U87, MCF-7 etc. (Roshini et al., 2017). Moreover they can accumulate in various internal organs (such as liver, spleen, lungs, kidney, and heart) *via* circulation and then produce adverse consequences (Shen et al., 2019).

Quantum dots (QDs) with a diameter of 1–10 nm, have unique optical properties, such as broad excitation, narrow emission spectra, and long fluorescence lifetimes (Yaghini et al., 2018; Lu et al., 2019; Touaylia and Labiadh, 2019). These advantages make QDs attractive for biomedical applications, including fluorescent probes, clinical diagnostic, and therapeutic tools (Yaghini et al., 2018). Commercially available cadmium-based QDs release toxic cadmium ions, which

limit their future applicability, particularly in view of environmental regulations (Sudhagar et al., 2011; Aboulaich et al., 2012). ZnO QDs are promising and have received much attention because of their Cd-free, inexpensive, and excellent optical properties (Roshini et al., 2017). The widespread application inevitably cause the increased release into the environment. Therefore, it is necessary to evaluate the potential toxic effects of ZnO QDs.

Our previous studies have demonstrated that ZnO QDs are located in the mitochondria, disrupt the activity of anti-oxidative enzymes, and induce oxidative stress after intravenous injection in mice (Yang et al., 2014b). In this study, we assessed the cytotoxicity of ZnO QDs in HeLa cervical cancer cell and HEK-293T human embryonic kidney cell lines, and investigated the potential effect on reactive oxygen species (ROS) production, loss of mitochondria membrane potential (MMP), and promotion of apoptosis.

MATERIALS AND METHODS

Materials

Fetal bovine serum was purchased from Hyclone (Logan, UT, USA). Dimethyl sulfoxide was purchased from Sigma-Aldrich (St Louis, MO, USA). Dulbecco's modified Eagle's medium (DMEM), phosphate-buffered saline (PBS), and trypsin were purchased from Corning (New York, NY, USA). TRIzol reagent was purchased from Invitrogen (Carlsbad, CA, USA). Cell Counting Kit-8 (CCK-8), ROS color reagent 2',7'-dichlorodihydrofluorescein diacetate (DCFH-DA), and 5,5,0,6,6,0-tetrachloro-1,10,3,30-tetraethylbenzimidazol carbocyanine iodide (JC-1) were purchased from Beyotime (Shanghai, China). Deionized water was prepared from Millipore (Bedford, MA, USA). Other reagents used were of analytical grade.

The synthesis of ZnO QDs were as described previously (Yang et al., 2014a). The reaction was carried out at room temperature by consecutive dropwise addition of 450 ml 0.2 mol/L KOH in ethanol to 150 ml 0.1 mol/L ZnAc₂ in ethanol with stirring, and stirred for another 1 h. The obtained ZnO QDs was centrifuged and washed with absolute ethanol three times, then dried in vacuum. The characterization of ZnO QDs was described in **Supplemental Material**.

Cell Culture

HeLa and HEK-293T cells were cultured in DMEM containing 10% fetal bovine serum and 1% penicillin-streptomycin. The cell lines were maintained at 37°C in a humidity- and CO₂-controllable incubator (Thermo Forma, Marietta, OH, USA) with 5% CO₂. All the cell experiments were performed in a clean atmosphere.

Cell Viability Assay

Cell viability was determined by the CCK-8 assay. HeLa and HEK-293T cells were seeded into 96-well plates (2.0×10³ cells per well), and incubated at 37°C for 24 h. ZnO QDs in DMEM were

added at final concentrations of 25, 50, 100, 200, and 400 µg/ml. At the end of the fixed incubation period (6, 24, 48, and 72 h), cells were washed with PBS to remove excess QDs. We added 200 µl fresh medium and 20 µl CCK-8 reagent. After 2 h incubation at 37°C, absorbance at 450 nm was recorded using a microplate reader. All experiments were performed in triplicate.

Measurement of Reactive Oxygen Species Production

ROS were determined using DCFH-DA. A total of 5.0×10⁴ HeLa or HEK-293T cells per well were cultured with 0, 50, and 100 µg/ml ZnO QDs for 1, 2, 4, 6, and 24 h. Then added 10 µM DCFH-DA working solution, and the cells were incubated for 20 min at 37°C. The plates were rinsed with serum-free medium three times to remove DCFH-DA. Fluorescence intensity was detected using a microplate counter at an excitation wavelength of 488 nm and emission wavelength of 525 nm.

Measurement of MMP ($\Delta\Psi_m$)

Changes in MMP were detected using a mitochondrion-specific cationic dye JC-1. HeLa and HEK-293T cells were incubated with 0, 50, and 100 µg/ml ZnO QDs for 24 h. We added JC-1 working solution and incubated the cells at 37°C in the dark for 20 min. We rinsed the cells with JC-1-free working solution three times, and replaced it with serum-free medium. Fluorescence intensity was recorded using a microplate counter. Red emission were at excitation an wavelength of 525 nm and emission wavelength of 590 nm, indicating membrane-potential-dependent JC-1 aggregates in mitochondria, while green fluorescence was detected at excitation wavelength of 490 nm and emission wavelength 530 nm, indicating the monomeric form of JC-1 in the cytoplasm. Mitochondrial depolarization resulted in a decrease in the red/green fluorescence intensity ratio.

Total RNA Isolation and Quantitative Real-Time PCR Analysis of Apoptotic Markers

After incubation with control and 50 µg/ml ZnO QDs for 6 and 24 h, cells were collected. Total RNA was extracted using the TRIzol method and quantified by NanoDrop 2000 UV-Vis Spectrophotometer (Thermo Scientific, Wilmington, DE, USA). Total RNA (1 µg) was reverse transcribed to synthesize complementary DNA (cDNA) using the High Capacity cDNA Reverse Transcription kit (Applied Biosystems, Foster City, CA, USA). Then, the messenger RNA (mRNA) expression levels of apoptotic markers including *Bax*, *Bak*, *Bcl2*, *Bcl-xl*, *Casp3*, *Casp7*, *Casp9*, and *p53*, were assessed using quantitative real-time PCR. Real-time PCR was performed by the 7500HT Thermal Cycler and SYBR Green Master Mix (Applied Biosystems). Primers were designed following previous reports (Bai et al., 2015; Czemplik et al., 2016; Sun et al., 2016), and the primers were as follows: *Bax* forward primer: 5'-AGGGTTTCATCCAGGATCGAGCAG-3' and reverse primer: 5'-ATCTTCTTCCAGATGGTGAGCGAG-3', *Bak* forward primer: 5'-GGATTGGTGGGTCTATGTTTC-3' and reverse primer: 5'-TCTGGGATTCC TAGTGGTGT-3', *Bcl2* forward primer: 5'-GCTGAGGCAGAGGGTTATG-3' and reverse primer: 5'-GCCCCC TTGAAAAAGTTCAT-3', *Bcl-xl* forward primer: 5'-

GATCCCATGGCAGCAGTAAAGCAAG-3' and reverse primer: 5'-CCCCATCCCGGAAGAGTTCATTCAC-3', *Cap3* forward primer: 5'-AGCCCATTTCTCCATACG-3' and reverse primer: 5'-TTATTGCCTCACCACCTTTAG-3', *Caspase7* forward primer: 5'-CATGCGATCCATCAAGACCA-3' and reverse primer: 5'-GGAAGCACTGAAGAGCG-3', *Caspase9* forward primer: 5'-TTGTGGAAGCCAACCCTA-3' and reverse primer: 5'-GCCAAATCTGCATTTCCC-3', *p53* forward primer: 5'-ACATGACGGAGGTTGTGA-3' and reverse primer: 5'-CACCACCACACTATGTCG-3', β -*actin* forward primer: 5'-GGCGGACTATGACTTAGTTG-3' and reverse primer: 5'-AAACAACAATGTGCAATCAA-3'. All samples were analyzed in duplicate measuring both the gene of interest and internal control of β -*actin*. Dissociation curve analysis was performed after each quantitative real-time PCR. Each experiment contained three technical repetitions, and each gene was independently detected three times. The normalized expression of the target genes was calculated using $2^{-\Delta\Delta CT}$.

Apoptosis Measurement by Flow Cytometry

An Annexin V Apoptosis Detection Kit (Multisciences, Hangzhou, China) was utilized to measure apoptosis of HeLa and HEK-293T cells. After incubation with control and 50 μ g/ml ZnO QDs for 24 h, cells were washed, trypsinized, and resuspended in the binding buffer at a concentration of 10^6 cells/ml. We added fluorescein isothiocyanate-annexin V and propidium iodide, and incubated the cells in the dark for 15 min

at room temperature. Apoptotic rate was analyzed using flow cytometry.

Statistical Analysis

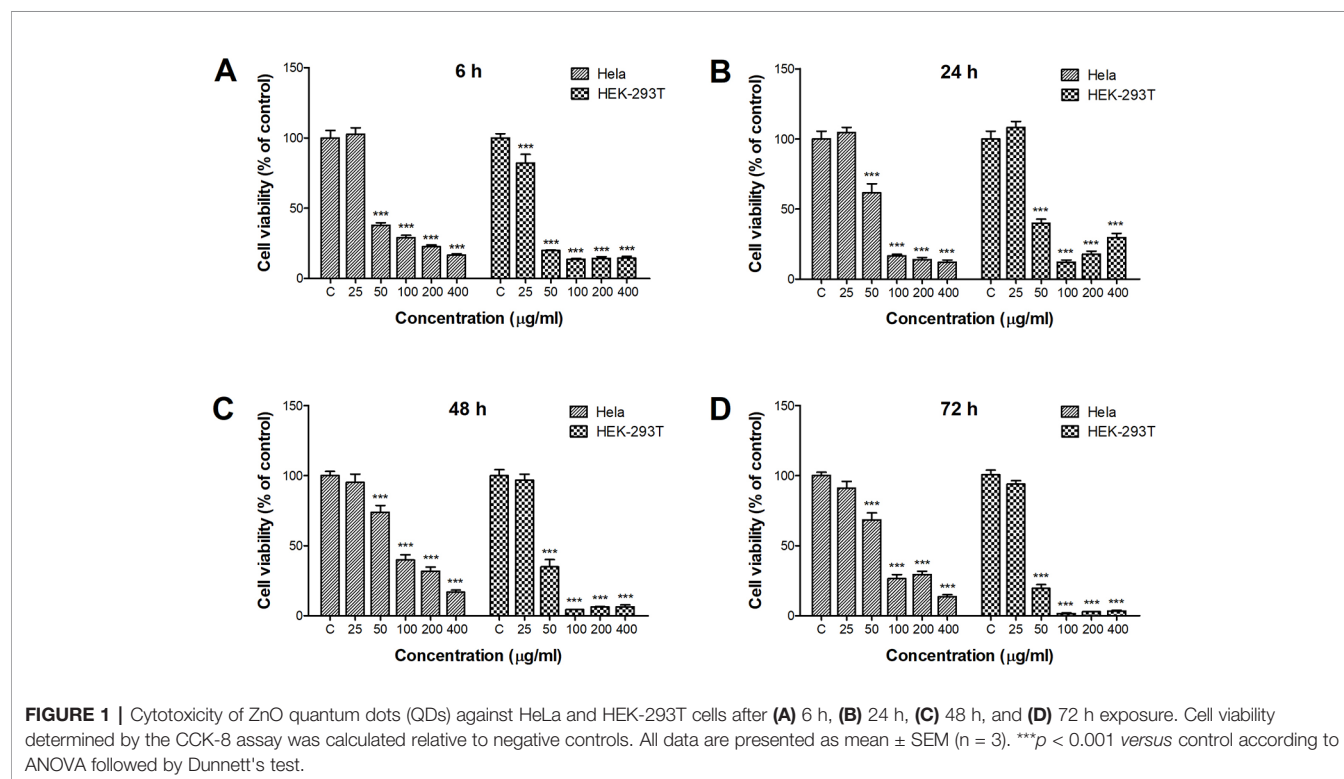
All the data are presented as mean \pm SEM. Multiple group comparisons of the means were evaluated by one-way analysis of variance (ANOVA) followed Dunnett's test using SPSS version 16.0. The unpaired t-test was used to test the difference between the two groups. $p < 0.05$ was considered statistically significant.

RESULTS

The average diameter of ZnO QDs was approximately 7.10 ± 0.30 nm according to transmission electron microscopy (TEM, **Figure S1**) and 7.43 nm from dynamic light scattering (DLS, **Figure S2A**). Zeta potential was -3.56 mV on the surface of ZnO QDs (**Figure S2B**). The UV-Vis absorption was located at 363 nm (**Figure S2C**) and their strong fluorescence centered at 552 nm (**Figure S2D**).

Cytotoxicity of ZnO Quantum Dots in HeLa and HEK-293T Cells

The CCK-8 assay was used to examine the viability of HeLa and HEK-293T cells after incubation with ZnO QDs (**Figure 1**). Obvious cytotoxicity was observed after only 6 h incubation with ZnO QDs (**Figure 1A**). Cell viability was decreased when the concentration of QDs increased. Significant cytotoxicity



appeared at a concentration of 50 $\mu\text{g/ml}$ in HeLa and HEK-293T cells, and the dosage was selected for following assays. The cytotoxicity of ZnO QDs in HEK-293T cells was greater than in HeLa cells. Incubation time did not significantly influence the viability of HeLa cells, while the viability of HEK-293T cells displayed a time-dependent decrease (Figures 1B–D).

Reactive Oxygen Species Induced by ZnO Quantum Dots

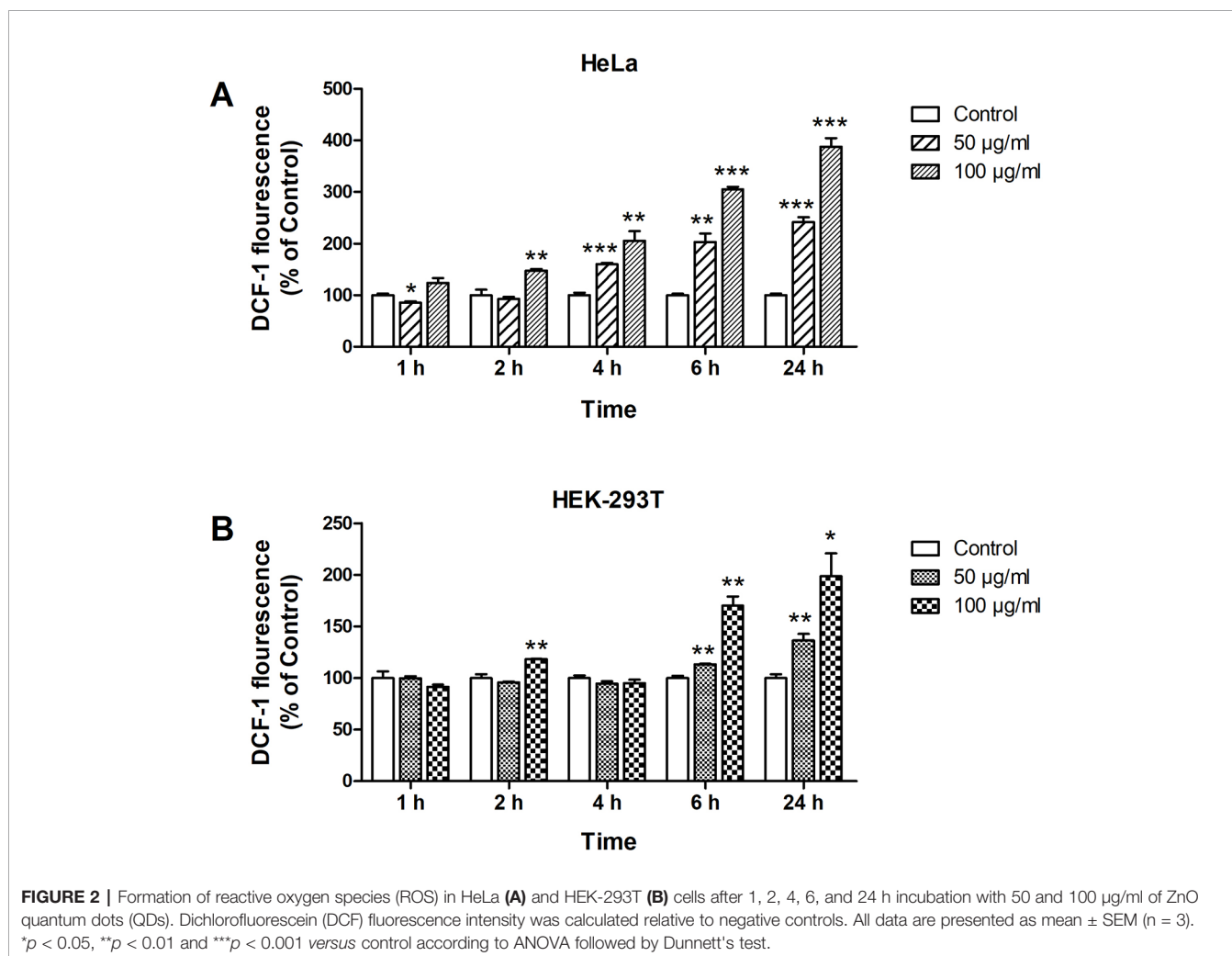
ROS generation by ZnO QDs was determined by DCF fluorescence. The fluorescence intensity were the same as control group until 4 h after ZnO QDs treated in HEK-293T cells (Figure 2B), which were significantly increased at 4 h in HeLa cell (Figure 2A). The fluorescence intensity induced by ZnO QDs at 100 $\mu\text{g/ml}$ was stronger than at 50 $\mu\text{g/ml}$ (dose dependent), and highest at 24 h (time dependent) in HeLa and HEK-293T cells. The fluorescence intensity in HeLa cells was stronger than in HEK-293T cells at the same incubation time and dose.

Loss of MMP Induced by ZnO Quantum Dots

We applied the fluorescent dye JC-1 to investigate the influence of ZnO QDs on $\Delta\Psi\text{m}$. When $\Delta\Psi\text{m}$ collapsed, JC-1 aggregates were unable to accumulate in the mitochondria and dissipated into JC-1 monomers, as a result of a decrease in the ratio of red to green fluorescence. The red/green ratio in HeLa cells was dramatically decreased from 3.77 ± 0.61 (control) to 0.70 ± 0.02 (50 $\mu\text{g/ml}$, $p < 0.001$) and 0.76 ± 0.01 (100 $\mu\text{g/ml}$, $p < 0.001$) after incubation with ZnO QDs for 24 h (Figure 3A). The red/green ratio was decreased from 1.94 ± 0.23 (control) to 0.17 ± 0.03 (50 $\mu\text{g/ml}$, $p < 0.001$) and 0.10 ± 0.01 (100 $\mu\text{g/ml}$, $p < 0.001$) in HEK-293T cells (Figure 3B).

Quantitative Real-Time PCR

We used quantitative real-time PCR to analyze the mRNA levels of apoptotic markers in HeLa and HEK-293T cells after incubation with 50 $\mu\text{g/ml}$ ZnO QDs for 6 and 24 h (Figure 4). At 6 h, only Bcl-2 (5.02-fold), caspase-9 (2.42-fold), and p53 (0.37-fold) were significantly altered in HeLa cells, while Bak



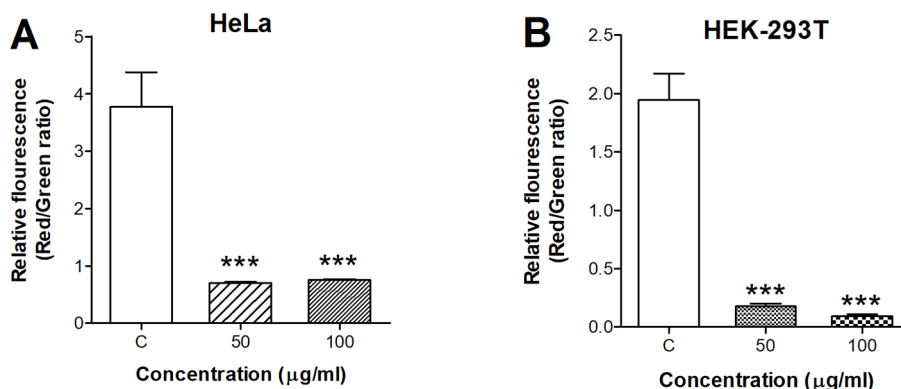


FIGURE 3 | Quantitative analysis of membrane potential after incubation with 50 and 100 µg/ml ZnO quantum dots (QDs) for 24 h. **(A)** HeLa and **(B)** HEK-293T cells. All data are presented as mean ± SEM (n = 3). ***p < 0.001 versus control according to ANOVA followed by Dunnett's test.

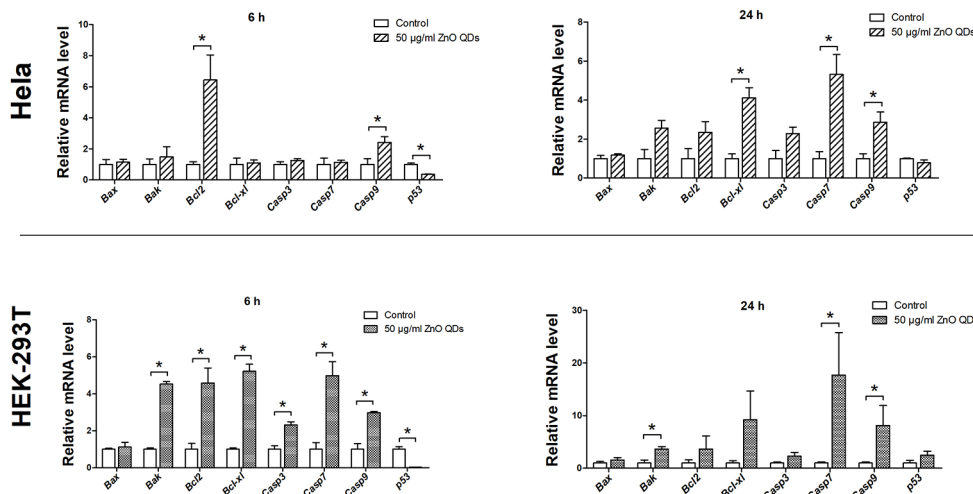


FIGURE 4 | Changes in messenger RNA (mRNA) expression levels of apoptotic markers in HeLa and HEK-293T cells after exposure to 50 µg/ml ZnO quantum dots (QDs) for 6 and 24 h. All data are presented as mean ± SEM (n = 3). *p < 0.05 according to the unpaired t-test between 50 µg/ml ZnO QDs and the control group.

(4.53-fold), Bcl-2 (4.58-fold), Bcl-xl (5.22-fold), caspase-3 (2.32-fold), caspase-7 (4.98-fold), caspase-9 (2.98-fold), and p53 (0.03-fold) were all significantly altered in HEK-293T cells. mRNA levels of caspase-7 and caspase-9 were increased in HeLa and HEK-293T cells after 24 h. At the same time, mRNA expression of p53 was similar to the control groups in HeLa and HEK-293T cells.

Apoptosis

The percentages of apoptotic and necrotic cells in HeLa (**Figure 5A**) and HEK-293T cells line (**Figure 5B**) were analyzed by flow cytometry. Incubation with 50 µg/ml ZnO QDs for 24 h significantly increased the percentage of early apoptotic cells

and late apoptotic cells in HeLa cells (**Figure 6A**). However, the cell population was located in late apoptosis in HEK-293T cells (**Figure 6B**). The total apoptosis ratio induced by ZnO QDs in HEK-293T cells (21.05 ± 4.81%) was higher than in HeLa cells (15.45 ± 1.30%). After treatment with 50 µg/ml ZnO QDs, necrotic cells remained at a low level in HeLa and HEK-293T cells.

DISCUSSION

In the present study, HeLa and HEK-293T cells were exposed to ZnO QDs (25, 50, 100, 200, and 400 µg/ml) for 6, 24, 48, and 72 h. The cytotoxicity was measured by CCK-8 assay. Cell viability was

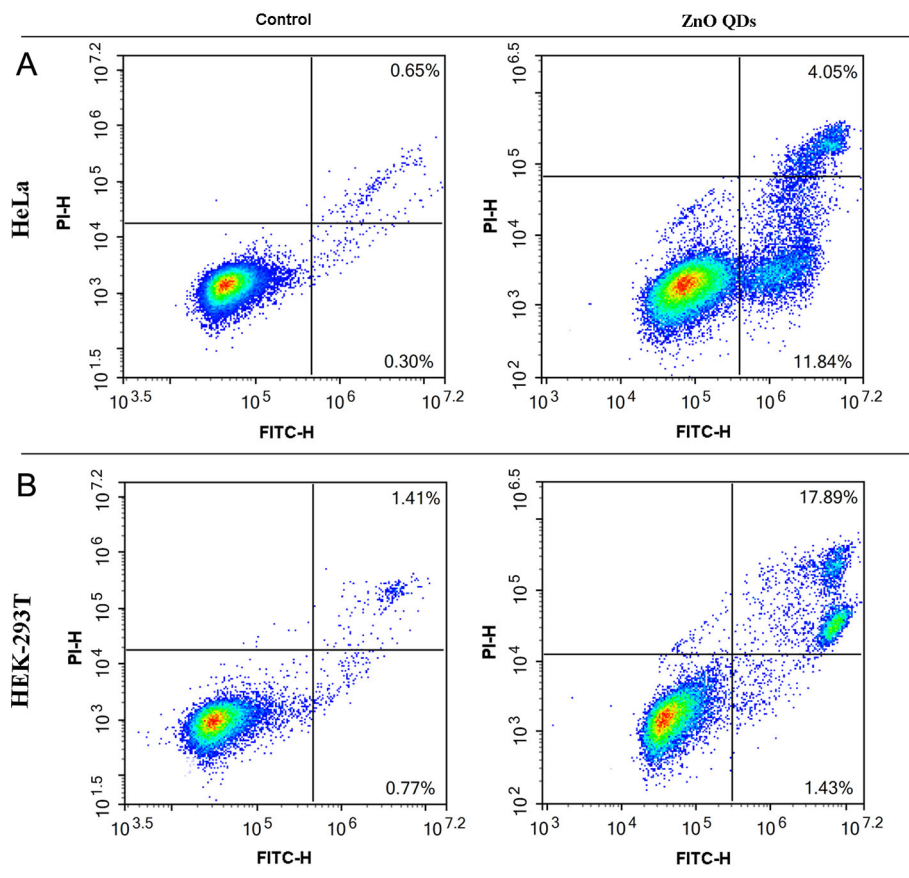


FIGURE 5 | Annexin V/PI staining combined with flow cytometry was used to determine apoptosis induced by 50 $\mu\text{g/ml}$ ZnO QDs treated for 24 h. **(A)** HeLa and **(B)** HEK-293T cells.

significantly reduced by 50 $\mu\text{g/ml}$ ZnO-QDs after only 6 h treatment. This is contradicted with the result of Sudhagar et al. reports, that ZnO QDs were biocompatible and non-toxic even at 100 $\mu\text{g/ml}$ for up to 48 h in MDA-MB-231 breast cancer cells (Sudhagar et al., 2011). In our study, the cytotoxicity of ZnO QDs in HEK-293T cells was greater than in HeLa cells. However, Roshini et al. reported that ZnO QDs showed less toxicity to HEK-293 cells but significantly induced cytotoxicity in human breast cancer cells (Roshini et al., 2017).

The release of ROS has been reported in cells exposed to ZnO nanoparticles, and involved in their toxic effects (Heim et al., 2015; Yang et al., 2015). Marfavi and Vallabani et al. demonstrated that ZnO NPs induced ROS in GBM U87MG and HaCaT cell line (Marfavi et al., 2019; Vallabani et al., 2019). In our study, the fluorescence intensity was increased as early as 4 h, which was consistent with the reports that ZnO NPs induces significant ROS in HaCaT cells after 3 h of treatment (Manna et al., 2015). ROS level increased in a time and dose-dependent manner, and was consistent with the result of CCK-8 assays (6 and 24 h). Therefore, we suggest that decreased cell viability was

related to oxidative stress. The free radicals would lead to disorganization of the cells, organelles and enzymes (Ahmad et al., 2015). Mitochondria are especially sensitive and vulnerable to cellular stress because of their high metabolic activity (Choi et al., 2007; Manna et al., 2015). We used a specific dye JC-1 for assessment of mitochondrial damage after exposure to ZnO QDs. We detected a decrease in MMP, suggesting an impairment of mitochondrial function. This is in according with the previous reports that ZnO NPs lead to mitochondrial membrane depolarization in HaCaT cells and human bone marrow-derived MSCs (Kim et al., 2019; Vallabani et al., 2019).

Both mitochondrial membrane depolarization and free radicals could trigger apoptosis *via* the intrinsic pathway. Upon quantification by flow cytometry, the total apoptosis ratio was significantly increased after exposure to 50 $\mu\text{g/ml}$ ZnO QDs as compared to the control group. Persaud and Kim et al. reported that ZnO NPs induced significantly late apoptosis at the concentrations of 20 $\mu\text{g/ml}$ (Kim et al., 2019; Persaud et al., 2019). Shen et al. revealed that ZnO NPs induced early and late apoptosis in low dosage, and mainly increased the late apoptosis in high dosage (Shen et al., 2019). In our

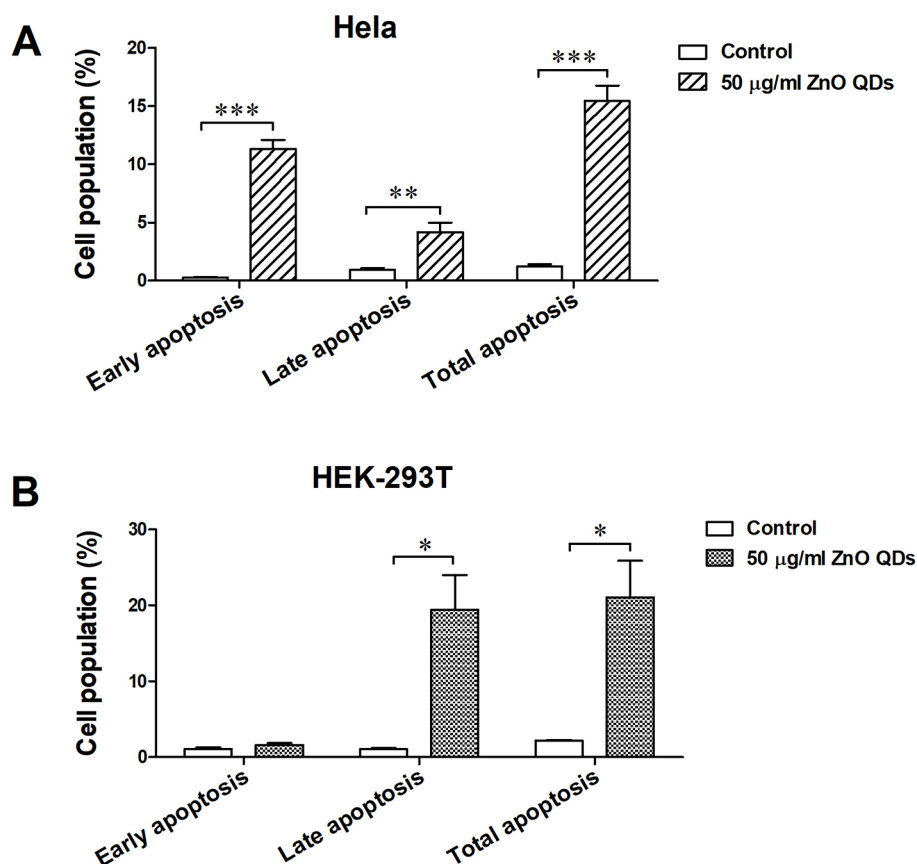


FIGURE 6 | Apoptotic rate of (A) HeLa and (B) HEK-293T cells after exposure to 50 µg/ml ZnO quantum dots (QDs) for 24 h. All data are presented as mean ± SEM (n = 3). * $p < 0.05$, ** $p < 0.01$ and *** $p < 0.001$ according to the unpaired t-test between 50 µg/ml ZnO QDs and the control group.

experiment, ZnO QDs increased early and late apoptosis in HeLa cells, but only late apoptosis in HEK-293T cells.

CONCLUSION

The cytotoxicity of ZnO QDs was evaluated in the HeLa and HEK-293T cell lines. ZnO QDs induced obvious cytotoxicity at a concentration of 50 µg/ml, and viability of HEK-293T cells was lower than that in HeLa cells. ROS level was increased in a time and dose-dependent manner by ZnO QDs and was consistent with the result of CCK-8 assays. Mitochondrial membrane depolarization and apoptosis occurred after exposure to ZnO QDs.

DATA AVAILABILITY STATEMENT

The datasets generated for this study are available on request to the corresponding authors.

ETHICS STATEMENT

The study was approved by the Committee of Medical Ethics and Welfare for Experimental Animals, Henan University School of Medicine.

AUTHOR CONTRIBUTIONS

SL and SJ developed the idea and designed the research. YY, ZS, WW and AX performed the experiments. YY analyzed the data and wrote the draft of the manuscript. SJ and SL contributed to revise the writing. All authors read and approved the submitted version.

FUNDING

This work was supported by research funds from the Key Science and Technology Program of Henan Province in China (Grant No. 182102310593, 192102310080), the National Natural Science Foundation of China (Grant No. 81600974, 81971280), the Key

Scientific Research Program for Universities of Henan Province (Grant No. 17A330001), the Key Science and Technology Program of Kaifeng City in China (Grant No. 1903083, 1903019, 1803034), and the Research Program for Young Talent of Henan University School of Medicine (Grant No. 2019018).

REFERENCES

- Aboulaich, A., Tilmaciu, C.-M., Merlin, C., Mercier, C., Guilloteau, H., Medjahdi, G., et al. (2012). Physicochemical properties and cellular toxicity of (poly) aminoalkoxysilanes-functionalized ZnO quantum dots. *Nanotechnology* 23, 335101. doi: 10.1088/0957-4484/23/33/335101
- Ahmad, J., Wahab, R., Siddiqui, M. A., Musarrat, J., and Al-Khedhairi, A. A. (2015). Zinc oxide quantum dots: a potential candidate to detain liver cancer cells. *Bioprocess Biosyst. Eng.* 38, 155–163. doi: 10.1007/s00449-014-1254-x
- Bai, H., Li, H., Li, W., Gui, T., Yang, J., Cao, D., et al. (2015). The PI3K/AKT/mTOR pathway is a potential predictor of distinct invasive and migratory capacities in human ovarian cancer cell lines. *Oncotarget* 6, 25520–25532. doi: 10.18632/oncotarget.4550
- Choi, A. O., Cho, S. J., Desbarats, J., Lovric, J., and Maysinger, D. (2007). Quantum dot-induced cell death involves Fas upregulation and lipid peroxidation in human neuroblastoma cells. *J. Nanobiotechnol.* 5, 1–1. doi: 10.1186/1477-3155-5-1
- Czemplik, M., Mierziak, J., Szopa, J., and Kulma, A. (2016). Flavonoid C-glucosides derived from flax straw extracts reduce human breast cancer cell growth *in vitro* and induce apoptosis. *Front. Pharmacol.* 7, 282. doi: 10.3389/fphar.2016.00282
- Heim, J., Felder, E., Tahir, M. N., Kaltbeitzel, A., Heinrich, U. R., Brochhausen, C., et al. (2015). Genotoxic effects of zinc oxide nanoparticles. *Nanoscale* 7, 8931–8938. doi: 10.1039/c5nr01167a
- Kim, D.-Y., Kim, J.-H., Lee, J.-C., Won, M.-H., Yang, S.-R., Kim, H.-C., et al. (2019). Zinc oxide nanoparticles exhibit both cyclooxygenase- and lipoxygenase-mediated apoptosis in human bone marrow-derived mesenchymal stem cells. *Toxicol. Res.* 35, 83–91. doi: 10.5487/tr.2019.35.1.083
- Lu, J., Tang, M., and Zhang, T. (2019). Review of toxicological effect of quantum dots on the liver. *J. Appl. Toxicol.* 39, 72–86. doi: 10.1002/jat.3660
- Manna, A., De Sarkar, S., De, S., Bauri, A. K., Chattopadhyay, S., and Chatterjee, M. (2015). The variable chemotherapeutic response of Malabaricone-A in leukemic and solid tumor cell lines depends on the degree of redox imbalance. *Phytomedicine* 22, 713–723. doi: 10.1016/j.phymed.2015.05.007
- Marfavi, Z. H., Farhadi, M., Jameie, S. B., Zahmatkeshan, M., Pirhajati, V., and Jameie, M. (2019). Glioblastoma U-87MG tumour cells suppressed by ZnO folic acid-conjugated nanoparticles: an *in vitro* study. *Artif. Cells Nanomed. Biotechnol.* 47, 2783–2790. doi: 10.1080/21691401.2019.1577889
- Persaud, I., Raghavendra, A. J., Paruthi, A., Alsaleh, N. B., Minarchick, V. C., Roede, J. R., et al. (2019). Defect-induced electronic states amplify the cellular toxicity of ZnO nanoparticles. *Nanotoxicology*, 1–17. doi: 10.1080/17435390.2019.1668067
- Roshini, A., Jagadeesan, S., Cho, Y.-J., Lim, J.-H., and Choi, K. H. (2017). Synthesis and evaluation of the cytotoxic and anti-proliferative properties of ZnO quantum dots against MCF-7 and MDA-MB-231 human breast cancer cells. *Mater. Sci. Eng. C. Mater. Biol. Appl.* 81, 551–560. doi: 10.1016/j.msec.2017.08.014
- Sharma, V., Anderson, D., and Dhawan, A. (2012). Zinc oxide nanoparticles induce oxidative DNA damage and ROS-triggered mitochondria mediated apoptosis in human liver cells (HepG2). *Apoptosis* 17, 852–870. doi: 10.1007/s10495-012-0705-6
- Shen, J., Yang, D., Zhou, X., Wang, Y., Tang, S., Yin, H., et al. (2019). Role of autophagy in zinc oxide nanoparticles-induced apoptosis of mouse LEYDIG cells. *Int. J. Mol. Sci.* 20, 4042. doi: 10.3390/ijms20164042
- Song, W.-J., Jeong, M.-S., Choi, D.-M., Kim, K.-N., and Wie, M.-B. (2019). Zinc oxide nanoparticles induce autophagy and apoptosis *via* oxidative injury and pro-inflammatory cytokines in primary astrocyte cultures. *Nanomaterials* 9, 1043. doi: 10.3390/nano9071043
- Sudhagar, S., Sathya, S., Pandian, K., and Lakshmi, B. S. (2011). Targeting and sensing cancer cells with ZnO nanoprobe *in vitro*. *Biotechnol. Lett.* 33, 1891–1896. doi: 10.1007/s10529-011-0641-5
- Sun, X., Liao, W., Wang, J., Wang, P., Gao, H., Wang, M., et al. (2016). CSTMP induces apoptosis and mitochondrial dysfunction in human myeloma RPMI8226 cells *via* CHOP-dependent endoplasmic reticulum stress. *BioMed. Pharmacother.* 83, 776–784. doi: 10.1016/j.biopha.2016.07.045
- Touaylia, S., and Labiadh, H. (2019). Effect of the exposure to Mn-doped ZnS nanoparticles on biomarkers in the freshwater western mosquitofish *Gambusia affinis*. *Int. J. Environ. Health Res.* 29, 60–70. doi: 10.1080/09603123.2018.1508648
- Vallabani, N. V. S., Sengupta, S., Shukla, R. K., and Kumar, A. (2019). ZnO nanoparticles-associated mitochondrial stress-induced apoptosis and G2/M arrest in HaCaT cells: a mechanistic approach. *Mutagenesis* 34, 265–277. doi: 10.1093/mutage/gez017
- Yaghini, E., Turner, H., Pilling, A., Naasani, I., and MacRobert, A. J. (2018). *In vivo* biodistribution and toxicology studies of cadmium-free indium-based quantum dot nanoparticles in a rat model. *Nanomedicine* 14, 2644–2655. doi: 10.1016/j.nano.2018.07.009
- Yang, Y., Lan, J., Xu, Z., Chen, T., Zhao, T., Cheng, T., et al. (2014a). Toxicity and biodistribution of aqueous synthesized ZnS and ZnO quantum dots in mice. *Nanotoxicology* 8, 107–116. doi: 10.3109/17435390.2012.760014
- Yang, Y., Zhao, T., Cheng, T., Shen, J., Liu, X., Yu, B., et al. (2014b). Hepatotoxicity induced by ZnO quantum dots in mice. *Rsc Adv.* 4, 5642–5648. doi: 10.1039/c3ra46583g
- Yang, X., Shao, H., Liu, W., Gu, W., Shu, X., Mo, Y., et al. (2015). Endoplasmic reticulum stress and oxidative stress are involved in ZnO nanoparticle-induced hepatotoxicity. *Toxicol. Lett.* 234, 40–49. doi: 10.1016/j.toxlet.2015.02.004

SUPPLEMENTARY MATERIAL

The Supplementary Material for this article can be found online at: <https://www.frontiersin.org/articles/10.3389/fphar.2020.00131/full#supplementary-material>

Conflict of Interest: The authors declare that the research was conducted in the absence of any commercial or financial relationships that could be construed as a potential conflict of interest.

Copyright © 2020 Yang, Song, Wu, Xu, Lv and Ji. This is an open-access article distributed under the terms of the Creative Commons Attribution License (CC BY). The use, distribution or reproduction in other forums is permitted, provided the original author(s) and the copyright owner(s) are credited and that the original publication in this journal is cited, in accordance with accepted academic practice. No use, distribution or reproduction is permitted which does not comply with these terms.